Numerical Modelling of Floor Deformation Mode at Longwall Face

J.A. Nemcik[1], B. Indraratna[2], N. Aziz[3] and W.J. Gale[4]

[1]Strata Control Technology,
PO Box 824, Wollongong East, NSW 2520, Australia
[2]Department of Civil & Mining Engineering
University of Wollongong, NSW 2522, Australia
[3]Department of Civil & Mining Engineering
University of Wollongong, NSW 2522, Australia
[4]Strata Control Technology,
PO Box 824, Wollongong East, NSW 2520, Australia

Abstract: High stress concentrations ahead of the longwall face often exceed the floor strength and induce fractures in the floor strata. While concentrations of the vertical stress alone induces fractures in the roof ahead of the longwall face, combinations of the vertical and horizontal stress appear to be the dominant factor in formation of floor fractures. These fractures develop in response to the triaxial stress conditions exceeding rock strength. In the immediate floor, fractures appear to form at frequent intervals dipping under the goaf at a steep angle while more complex bedding shear appears to dominate the floor failure at a greater depth. In a stronger floor the fractures appear to occur less frequently. If weak bedding planes are present in the floor, shear failure along these beddings can occur far ahead of the longwall face. The post failure displacements along the fractures and the formation of new fracture surfaces often occur in response to the stress relief, bending or buckling of thin bedded layers in the floor. The post failure displacements can be large and may interfere with mining operations. This paper presents the computational approach using FLAC to model the development of fractures in the floor strata. The model uses programmable "fish routines" that allow simulation of failure modes that may occur in response to the changing stress field ahead of the longwall face. Continuous monitoring of the two dimensional stress field is used to predict the fracture types and the direction at which the fractures may propagate. The fractures are then simulated using FLAC ubiqitous elements that allow to assign the joint direction and the reduction of joint strength in the direction of the calculated fracture. The stress state is tested continuously during the execution of the program and fractures are simulated when the stress exceeds the rock strength. This procedure can simulate the progressive development of fractures during the longwall advance. The method is particularly helpful to estimate the type of fractures and their frequency that depend on the strength of floor strata and stress build up during a longwall advance. The depth of floor failure can have a significant influence on the gas release from the floor strata in gaseous mines. The type of fractures and the fracture orientation that is computed can be presented in the movie files to view the development of fractures in the floor during the longwall advance.

Key Words: floor failure, longwall face, numerical model

Introduction

The underground observations by the authors indicate that in most cases failure of the intact floor strata occurs ahead of the longwall face. The frequency of the fractures appear to be related to the strength of floor strata. The observed mining induced fractures in the upper floor appear to be parallel to the longwall face dipping at steep angles towards the goaf. In a weakly bedded strata, slip along the bedding plane was often observed where fractured floor was exposed. The upper slip surface appears to experience greater displacements towards the goaf than the lower surface indicating that the shear displacement is consistent with bending of the floor and the stress relief towards the opening.

The complexity of stress build up during the progressive mining of the longwall face and the diversity of the bedded floor strata can make conventional predictions of the floor failure mechanism difficult. Current advances in the numerical modelling field enables simulation of complex strata behaviour and allows prediction of fracture development in the floor.

The aim of the conceptual model presented here is to develop the understanding of the early fracture development in the longwall floor and to compare the results with the underground observations. The Fast Lagrangian Analysis of Continua (FLAC) program was selected to simulate the development of fractures at a longwall face. The programmable "fish" routines within FLAC enable simulation of the fractures using well known rock failure modes. The rock strength, bedding strength and the state of the ground stress are the key factors influencing the floor failure.

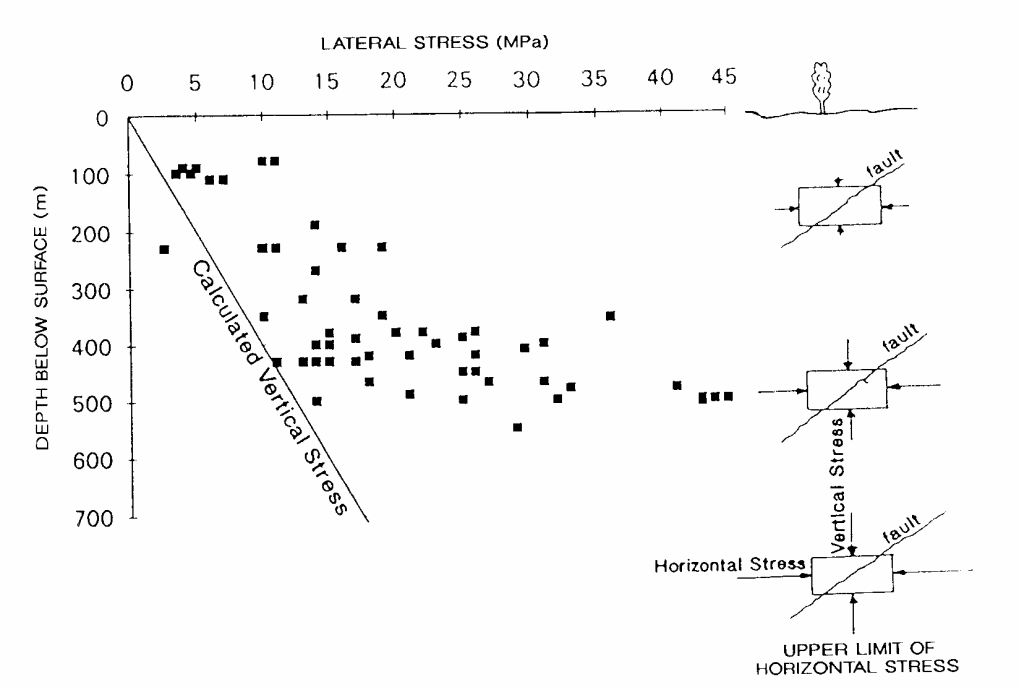

Fig. 1 – Increase of horizontal stress with depth in Australian coal mines as meassured underground.

Effect of Stress Field on Floor Failure

Underground measurements in Australia and overseas indicate that in most cases the lateral stresses are larger than the vertical stress. High lateral stresses are primarily the function of the tectonic movement in the region while the vertical stress is predominantly a function of the overburden weight. The ability of strata to transmit lateral stress increases with depth as the increase in confinement stresses prevent movement along the fault planes. This mechanism accounts for the lateral stress increase with depth of cover that has been measured in many parts of the world. The increase of lateral stress with depth as measured in many mines by SCT are presented in Figure 1. Concentrations of these stresses typically occur about mining excavations. While the concentrations of vertical stress alone induce fractures within the roof ahead of the longwall face,a combination of vertical and horizontal stress concentrations appear to be the dominant factor in the initial fracture development below the longwall floor.

Vertical Stress at Longwall Face

Vertical stress concentrations at a longwall face occur as the goaf formation takes place. The undermined overburden strata tend to overhang at the excavation edges while the caving occurs further away from the edge. Caving of strata behind the moving longwall supports is illustrated in Figure 2. The subsidence profiles (Holla,1985) indicate that a typical overhang of strata at the surface in relation to the goaf edge is approximately equal to 0.6 to 0.7 times the depth of cover. Magnitude of the vertical stress varies along the length of face and is approximately at its maximum at or near the centre of the longwall.

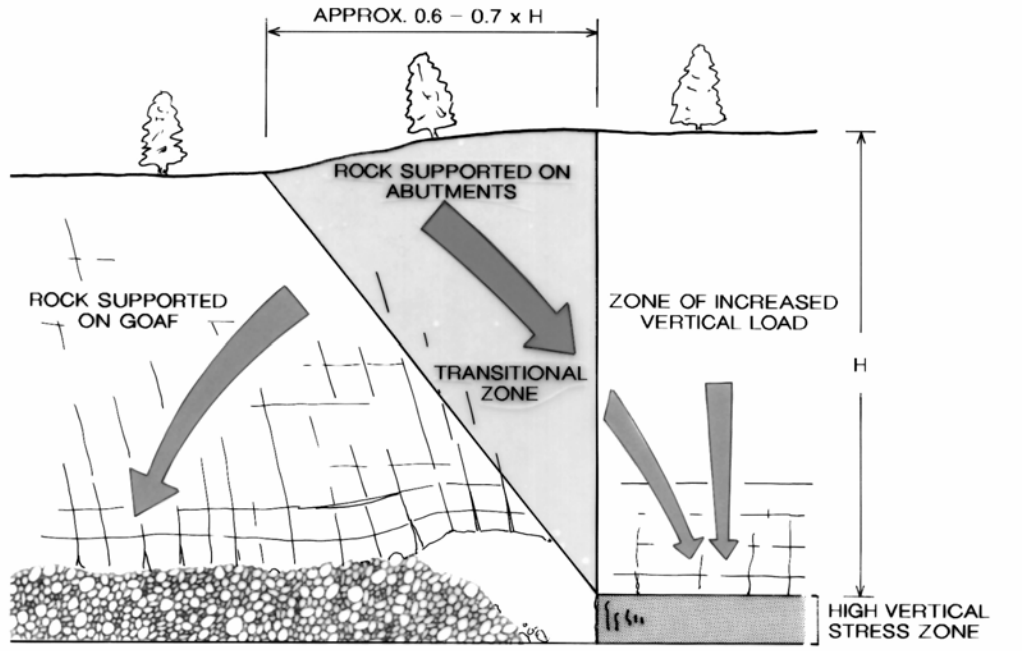

Fig. 2 – Vertical stress at the longwall face.

The longwall is said to be supercritical in width if the vertical stress at the centre of longwall is not influenced by the chain pillars located at the sides of the longwall panel. The subsidence profiles indicate that the longwalls are supercritical when the face is wider that approximately 1.2 to 1.4 times the depth of cover. In the case of the supercritical panel width, the front abutment at the centre of longwall will carry a maximum possible load which consists of the original in-situ virgin stress and the portion of the overhanging goaf strata. Shearing of the vertical load between the side pillars, goaf and the front of the longwall face occurs when the longwall is of a subcritical width. Majority of Australian longwalls are of a subcritical width. The stress concentrations that cause floor failure increases with depth and therefore, most of the affected longwalls would be of a sub-critical width.

Numerical models (Gale at al, 1998) and microseismic measurements (Kelly at al, 1998) indicate that two factors that control the peak stress concentrations ahead of the longwall face are the depth of cover and the modes of roof failure. Typically, when mining in weak ground, roof failure tends to develop ahead of the longwall face thus reducing peak stress concentrations and redistributing the stresses further ahead of the longwall face.

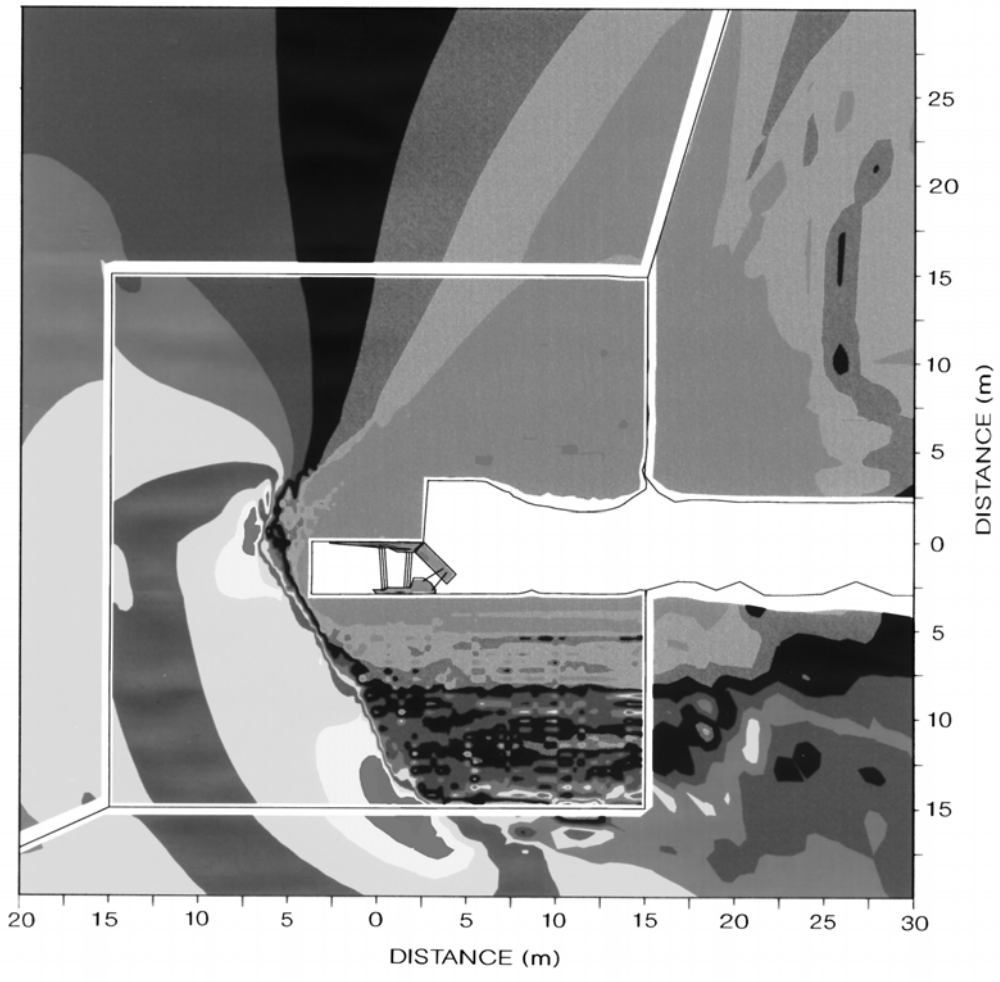

Fig. 3 – Concentrations of maximum stress ahead of fractured floor.

Lateral Stress at Longwall Face

It is usual practice to orient longwall gateroads at a low angle to the maximum principal horizontal stress σ_1 to prevent damage to the roadways and to avoid large stress concentrations at the longwall corners. The high lateral stresses are therefore oriented at a high angle to the longwall face. During longwall operations, strata above the seam experience lateral stress relief towards the goaf. This relief has been measured in many Australian coal mines (Matthews at al, 1992). The roof strata and the coal face experiencing the lateral stress relief are relatively free to expand towards the goaf opening as there are virtually no reaction forces to resist this movement. As the depth below the floor increases, the floor regains the ability to carry the lateral stress. The concentrated vertical and horizontal stresses combine to form a typical high stress zone in the floor ahead of the fractured zone as shown in Figure 3, where the maximum stress concentrated 15m below the powered supports.

Underground observations indicate that the floor failure appears to occur mainly at or near the centre of the longwall face, and implies that the combination of the stress relief towards the longwall opening and the vertical stress concentrations have a significant influence on the floor failure.

Modelling Approach

Strata behaviour at the longwall face was modelled using Fast Lagrangian Analysis of Continua (FLAC) to investigate parameters contributing to the floor failure. (Details about FLAC modelling are discussed in the FLAC manual Version 3.2, ITASCA 1993). A computational model was constructed to simulate a retreating longwall face.

The large scale geometry was modelled to establish appropriate stressfields at the longwall face area. The grid extended from the surface to 200m below the seam. The 330m wide section incorporated the coal seam sandwiched between the homogeneous rock layers. The model was gravity loaded to simulate vertical stress. To ensure that vertical stress at longwalls of subcritical width corresponded to the stress expected at the centre of the longwall face, the longwall excavation was stopped when the reflective boundary at the consolidated goaf edge was approximately at the distance of one half the longwall width. This technique was validated by underground stress measurements (Gale at al,1998). The virgin lateral stress of 1.5 times the vertical stress was used in the roof and floor layers while the lateral stress in the seam was scaled down according to the coal stiffness.

The true behaviour of strata can be achieved only if underground mining is simulated in detail. Rock failure develops in response to a change in stress while stress redistribution occurs as rock fails. To simulate strata failure as normally experienced underground, the coal was excavated sequentially with 0.7m wide cuts to simulate longwall advance. The rock was allowed to fail and the stresses redistributed before proceeding to the next cut.

The model uses programmable fish routines developed by SCT that allow simulation of failure modes in response to changing stress fields. Continuous monitoring of the two dimensional stress field was used to predict the fracture types and the direction at which fractures may propagate. The fractures were then simulated by assigning new directions and the post failure properties to the ubiquitous joints embedded in each grid zone. The stress state was tested continuously and fractures simulated when stress exceeded the rock strength. This procedure can simulate the progressive development of fractures during the longwall advance.

Numerical Model

The rock properties used in the model were based on the triaxial tests of overburden rock and coal in the Illawarra region as given in Table 1 below.

Table 1 Rock Properties used in the Model

Rock	Floor		Coal		Roof		Weak Bedding	
Bulk Modulus (GPa)	7		3		7		5	
Shear Modulus (GPa)	5		2		5		3.6	
Cohesion (MPa)	6		0.5		6		2	
Intact Friction	35°		35°		35°		25°	
Resid Friction	38°		35°		38°		25°	
Max tension (MPa)	2		0.5		2		0.5	
Ubiquitous Joint Cohesion (MPa)	Intact 6	Residual 0	Intact 6	Residual 0	Intact 6	Resid 0	Intact 1	Residual 0
Ubiquitous Joint Friction (Deg)	Intact 38	Residual 38	Intact 35	Residual 35	Intact 38	Resid 38	Intact 25	Residual 25
Confining Stress (MPa)	Intact Strength (MPa)	Residual Strength (Mpa)	Intact Strength (MPa)	Residual Strength (MPa)	Intact Strength (MPa)	Resid Strength (Mpa)	Intact Strength (MPa)	Residual Strength (Mpa)
0	60	0.05	12	0.05	60	0.05	20	0.05
1	75	15	18	8	75	10	22	2.5
2	82	22	23	11	80	15	25	5
5	100	40	35	23	92	27	30	10
10	130	70	53	41	108	43	35	15
20	190	130	70	58	140	75	50	30

The model of the longwall supports was constructed using the grid and the support elements. The canopy stiffness was varied to simulate the properties of the actual longwall support in use. The modelled supports were advanced forward and reset each time the coal was cut. The set loads were gradually increased to the yield value in response to the support convergence.

The goaf behind the supports was allowed to fall freely for 2m to reach the zone where a vertical load was applied to the goaf roof.

Concentration of the Maximum Stress

The models indicated that a large portion of the roof above and behind the longwall is severely fractured and cannot transmit stress. The redistribution of the insitu stresses occur ahead of the fractured zone and the stresses concentrate adjacent to the excavation edges where the rock is intact. The lateral stresses that were transmitting through the roof strata take a new path dipping into the floor. All models indicated that maximum stress was concentrated ahead of the floor failure below the longwall face. A typical location of the maximum stress is displayed 15m below the longwall supports in a stress contour plot shown earlier in Figure 2.

Fracture Mode Ahead of the Longwall Face

The four major types of strata failure that were simulated in the model included: intact shear, intact bedding shear, tension crack, bedding tension and the residual failure along the existing fractures.

The intact shear strength used, where the rock fractures are typically oriented at an angle of $\pi/4-\phi/2$ from the maximum stress direction, is given in Table 1. (Brady and Brown, 1985).

The shear strength was calculated for each grid zone within the model. The known stress state was used to constantly update safety factors for each grid zone. Similarly, the intact bedding shear strength and the maximum tensile strength of rock were also compared to the stress fields and the safety factors for each grid zone were constantly evaluated. When any or all of the safety factors fell below unity, the lowest safety factor was chosen, the fracture direction calculated, the ubiquitous joint oriented in the direction of the fracture and the post failure properties assigned to the joint. Further calculations of the displacements and stresses along the modified ubiquitous joints simulated propagation of fractures through the floor.

Floor Failure Observed in the Model

The floor failure was examined when the longwall excavation retreated to the desirable location. The failure zones shown in Figure 4 appeared to propagate deep into the floor. The maximum stress direction ahead of the broken floor was steeply dipping towards the goaf as shown in Figure 5. Even though the overall direction of the failure zones propagated downwards at a steep angle, the actual orientation of fractures appeared to be dipping at a shallower angle. The model indicated that each failure zone was formed from a series of parallel fractures oriented at $\pi/4-\phi/2$ from the general direction of the maximum stress at the tip of the fracture. As the depth below the floor increased, the shear fractures within the steeply inclined failure zones appeared to fail parallel to the bedding planes.

The direction of calculated fractures at the floor level compared well with the dip of fractures observed in the mudstone floor exposed at the 500m deep longwall finish line. The observed mining induced fractures were parallel to the face, spaced at intervals of between 0.05m to 1m and were dipping at an angle of 70° to 90° towards the goaf. The photograph of the exposed floor fractures at the 500m deep longwall finish line is presented in Figure 6.

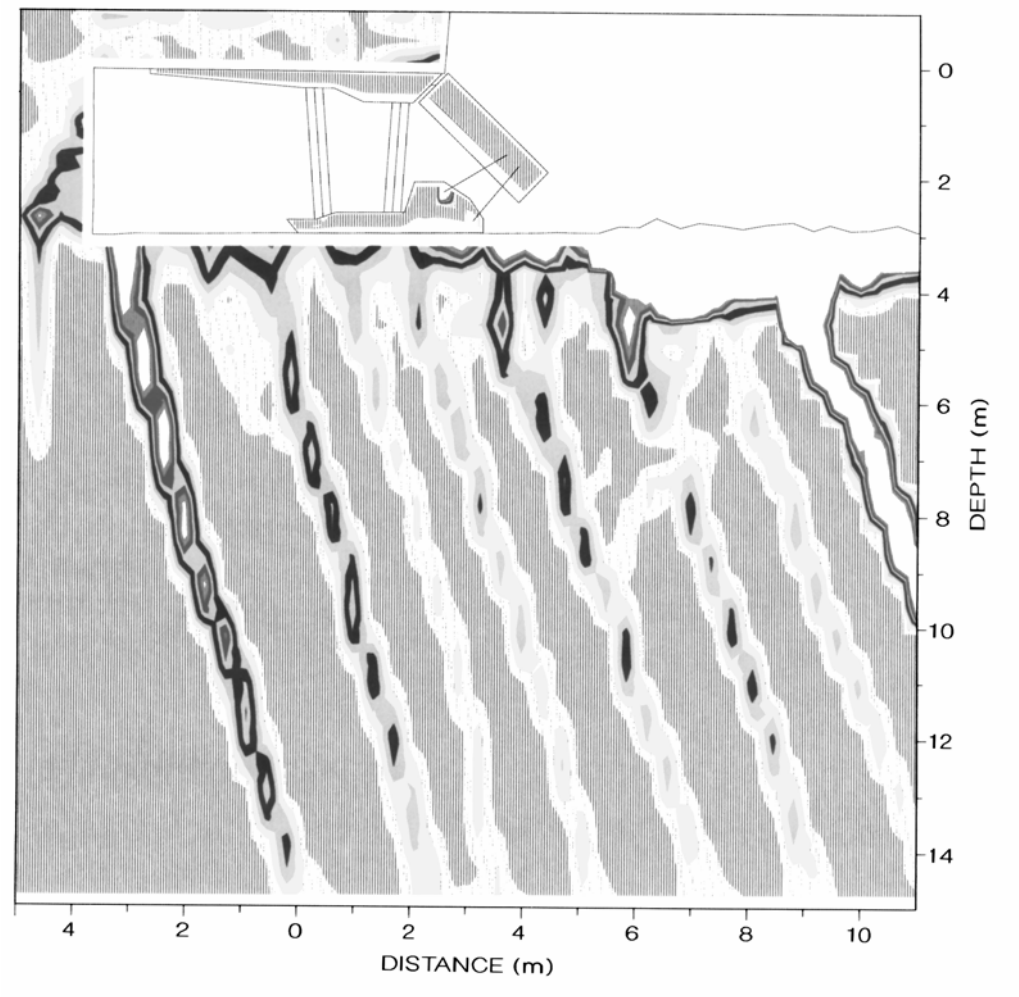

Fig. 4 – Shear zones in floor below the longwall face.

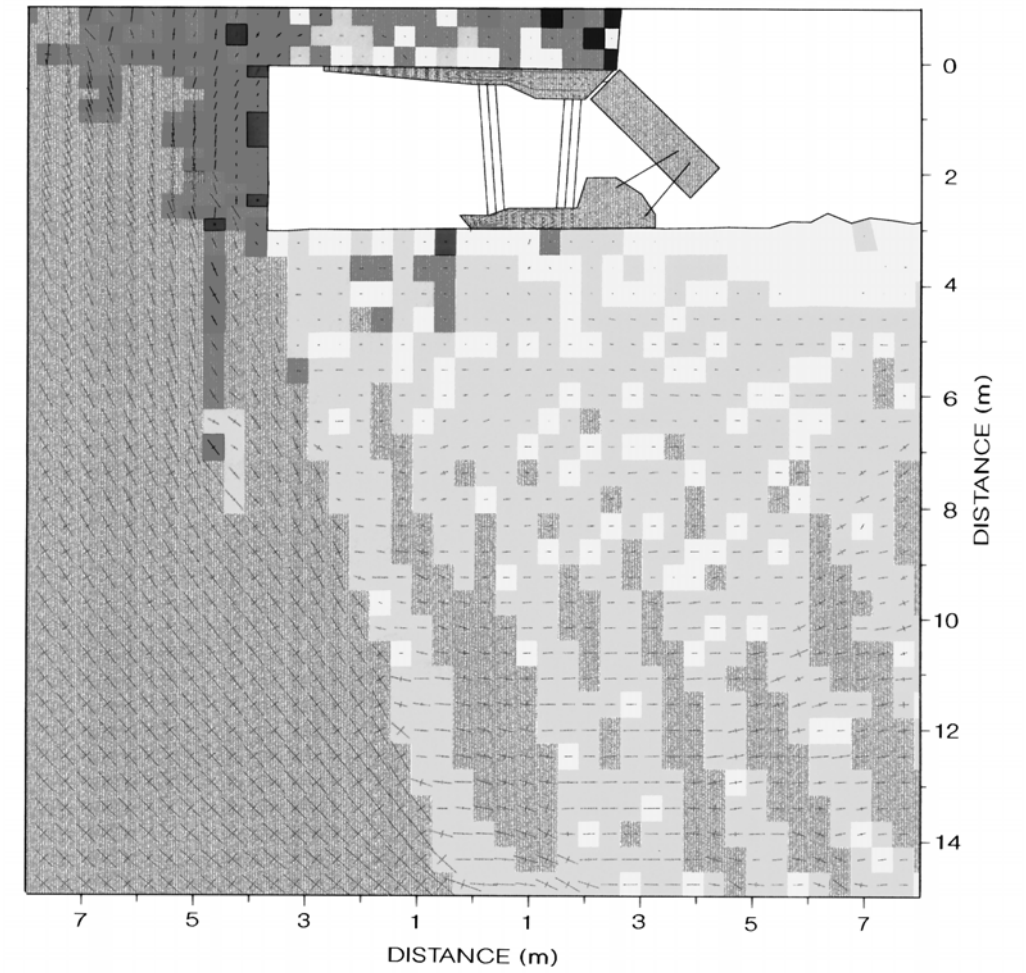

Fig. 5 – Mode of floor failure and principal stress vectors at a longwall face.

Fig. 6 – Photograph of mining induced fractures exposed at 500m deep longwall finish line.

Depth and Frequency of floor failure

The floor failure was modelled at the depth of 200m, 300m 400m and 500m. The depth of failure in a homogeneous rock increased with depth as shown in Figure 7. The influence of depth on floor failure cannot be generalised since the stress concentrations in the floor are often affected by roof failure. The complexity of the insitu strata behaviour suggests that the depth of floor failure cannot be predicted reliably without the use of the detailed computational model for the specific site.

The study indicated that the majority of fractures in the model developed either at every shear cut or at less frequent intervals. The frequency at which the failure zones propagated into the floor appeared complex and not directly related to the depth of cover.

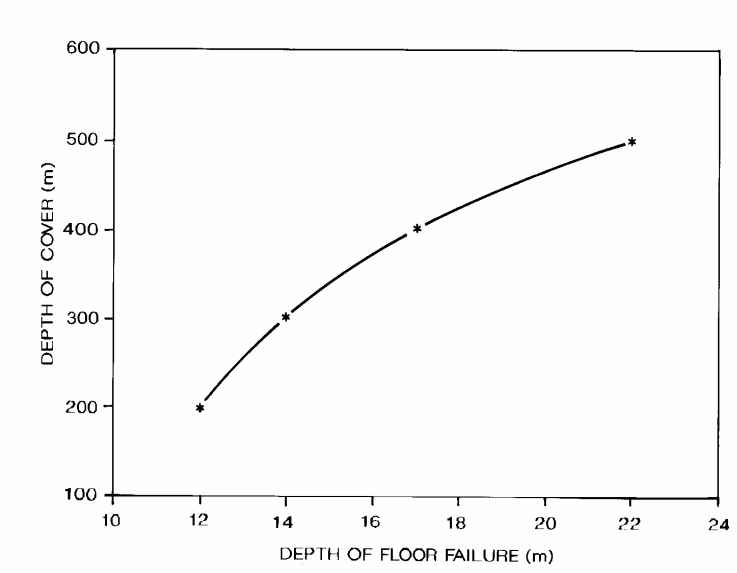

Fig. 7 – Modelled depth of floor failure for various depths of overburden cover.

Influence of Weak Bedding on Floor failure

Presence of weak bedding planes in the floor appear to dominate the floor failure ahead of the longwall face. When modelling a thin layer of weak rock located below the floor (Figure 8), failure propagated far ahead of the longwall face. The model indicated that the near vertical or near horizontal shear fractures developed within the weak bedding. As expected, failure of the weak bedding changed the principal stress directions in the floor below and allowed the upper floor displacement towards the longwall face. Failure of the horizontal bedding did not seem to affect the formation

of the subvertical floor failure zones. The fractured floor appeared to take the shape of large blocks separated by subvertical and horizontal fracture zones.

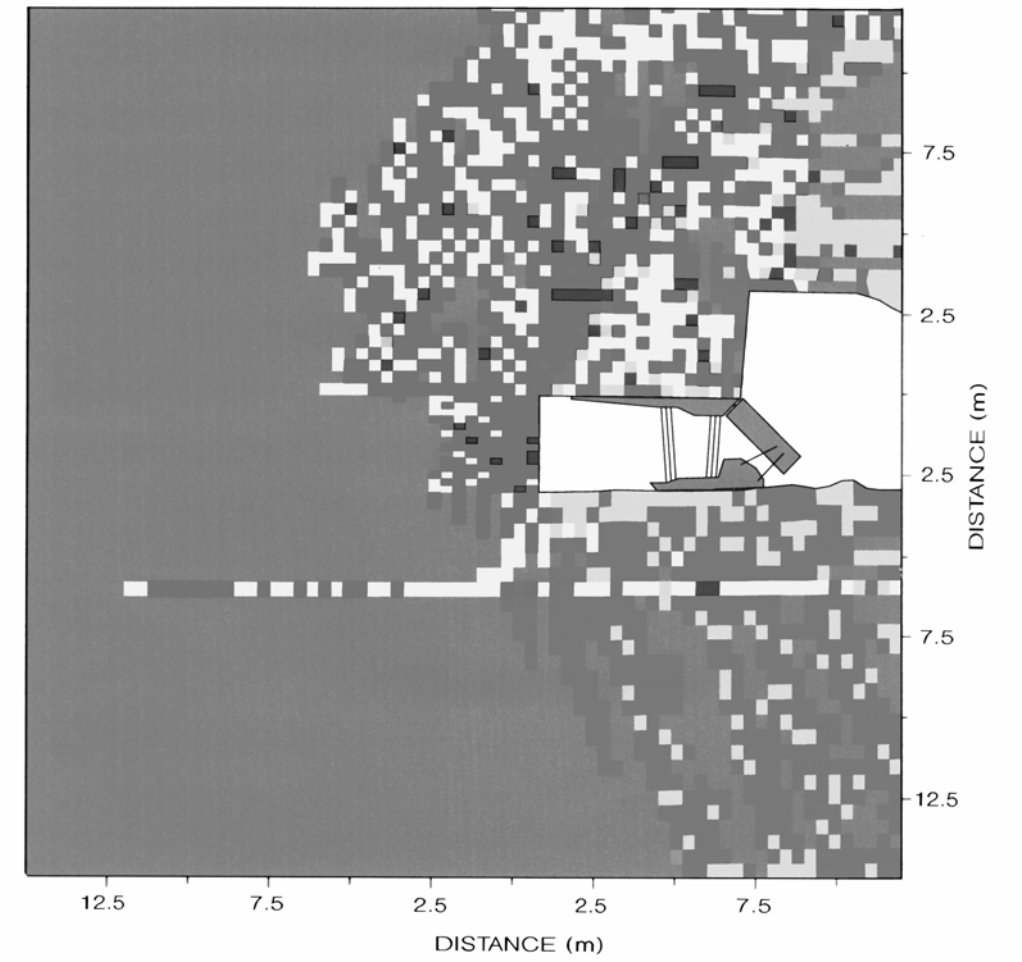

Fig. 8 – Model of weak bedding below floor.

Conclusions

In summary, this study shows the principles of floor failure mechanism based on numerical modelling and underground observations. The complexity of the insitu strata behaviour suggests that the floor failure cannot be predicted reliably without the use of the detailed computational model. Results from FLAC modelling indicate that the floor failure occurs at or ahead of the longwall face where the stresses are high. The maximum stress was found in the floor ahead of the fractured zones. The maximum stress direction was steeply dipping towards the goaf.

While the extent of floor failure is dependent on the magnitude of stress and strength of rock ahead of the longwall face, the direction of the principal stress and the bedding plane properties determine the type of fractures. The models support the existence of near vertical fractures observed in the floor at the longwall face. Even though the overall direction of the failure zones propagated downwards at a steep angle, the actual orientation of fractures appeared to be dipping at a shallower angle. The model indicated that each failure zone consists from a series of parallel fractures oriented at $\pi/4-\phi/2$ from the general direction of the maximum stress at the tip of the

fracture. The study shows that the presence of weak bedding planes in the floor dominate the floor failure ahead of the longwall face.

The progressive excavation of the modelled seam suggests that the primary floor failure is cyclic in nature where fracture zones develop after every shear is cut or less frequently when stress build up occurs. The stress distribution in the floor at the longwall face indicate that the powered supports do not appear to influence formation of the fractures in the floor ahead of the longwall face.

The depth of floor failure in the model increased with the depth of cover, however, the depth of floor failure cannot be generalised since the stress concentrations in the floor are often affected by roof failure. Development of the subvertical failure zones and failure along the bedding planes gives the floor strata a typical blocky appearance. The geometry of the floor failure and the depth of the subvertical fractured zones can have a significant influence on the gas release from the floor strata in gaseous mines.

The model of floor failure below the longwall face has proven to be of a significant value and further development is envisaged to continue.

References

Holla, L. 1985, The Minimisation of Surface Subsidence by Design of Mine Workings, Bulletin Proceedings, Australasian Institute of Mining and Metallurgy, Volume 290, No.6, September, 1985 pp.53-59.

Gale, W.J. and Nemcik, J.A., Prediction of Strata Caving Characteristics and its Impact on Longwall Operation, COAL98 Conference, University of Wollongong Press, pp. 156-166.

Kelly, M. Gale, W.J., Hatherly, P., Basulu, R. and Luo, X., Combining Modern Assessment Methods to Improve Understanding of Longwall Geomechanics, COAL98 Conference, University of Wollongong Press, pp. 523-535.

Matthews, S.M., Nemcik, J.A. and Gale W.J.,1992, Horizontal Stress Control in Underground Coal Mines, 11th International Conference on Ground Control in Mining, Wollongong, University of Wollongong Press, pp.289-296.

Itasca, 1993, Fast Lagrangian Analysis of Continua, FLAC User Manual, Verison 3.2, Itasca Consulting Group Inc., Minneapolis, Minnesota, USA.

Brady, B.H.G and Brown, E.T., 1985, Rock Mechanics for Underground Mining, Second Edition, Chapman and Hale, London, pp.105-125.